atmosphere

MDPI

Article

Tree-Ring Isotopes Provide Clues for Sink Limitation on Treeline Formation on the Tibetan Plateau

Xing Pu [1,2], Xiaochun Wang [3] and Lixin Lyu [1,*]

[1] State Key Laboratory of Vegetation and Environmental Change, Institute of Botany, Chinese Academy of Sciences, 20 Nanxincun, Haidian District, Beijing 100093, China; puxing201123@ibcas.ac.cn
[2] University of Chinese Academy of Sciences, Beijing 100093, China
[3] Key Laboratory of Sustainable Forest Ecosystem Management, Ministry of Education, School of Forestry, Northeast Forestry University, Harbin 150040, China; wangx@nefu.edu.cn
* Correspondence: lixinlv@ibcas.ac.cn; Tel.: +86-10-6283-6883

Abstract: Identifying what determines the high elevation limits of tree growth is crucial for predicting how treelines may shift in response to climate change. Treeline formation is either explained by a low-temperature restriction of meristematic activity (sink limitation) or by the photosynthetic constraints (source limitation) on the trees at the treeline. Our study of tree-ring stable isotopes in two Tibetan elevational transects showed that treeline trees had higher iWUE than trees at lower elevations. The combination of tree-ring $\delta^{13}C$ and $\delta^{18}O$ data further showed that photosynthesis was higher for trees at the treeline than at lower elevations. These results suggest that carbon acquisition may not be the main determinant of the upper limit of trees; other processes, such as immature tissue growth, may be the main cause of treeline formation. The tree-ring isotope analysis ($\delta^{13}C$ and $\delta^{18}O$) suggests that Tibetan treelines have the potential to benefit from ongoing climate warming, due to their ability to cope with co-occurring drought stress through enhanced water use efficiency.

Keywords: alpine treeline; water use efficiency; elevation; tree rings; stable isotopes; sink limitation

check for updates

Citation: Pu, X.; Wang, X.; Lyu, L. Tree-Ring Isotopes Provide Clues for Sink Limitation on Treeline Formation on the Tibetan Plateau. *Atmosphere* **2021**, *12*, 540. https://doi.org/10.3390/atmos12050540

Academic Editors: Achim Bräuning and Chuixiang Yi

Received: 1 April 2021
Accepted: 18 April 2021
Published: 23 April 2021

1. Introduction

Understanding what determines the high elevation limits of trees is crucial for predicting how treelines may shift in response to climate change. On a global scale, low temperature is found to impact the growth and regeneration of forests at the treeline [1–3]. The low temperature limitation on tree metabolism is related to either carbon gain or photosynthesis, known as the "source limitation hypothesis" [4–6], or tissue formation, known as the "sink limitation hypothesis" [7,8].

Carbohydrate concentrations of trees have been used to test these two hypotheses [9–11]. If treeline trees are able to acquire photoassimilates more efficiently than they can be used for growth, carbohydrates would accumulate in tissues, and, therefore, trees would have more available carbon (non-structural carbon, "NSC") than sinks are able to consume [7,12]. Evidence for the sink limitation hypothesis would be the following scenario: the carbohydrate reserves of treeline trees are not severely depleted at any time of the year, and the carbohydrate concentrations are higher in trees growing at the treeline than in trees growing at lower altitudes in the Himalayas [13,14]. Otherwise, the source limitation hypothesis would be supported. In addition to direct measurements of the NSC of tree tissues, carbon sink–source relationships have been studied using manipulation experiments [6,15–17]. One way to reduce the strength of sinks in trees is to remove buds [4,15]. Similarly, the sources can be manipulated, either by increasing the CO_2 concentration of air [18,19] or by removing the photosynthetically active tissues, such as defoliation [15,16,20,21].

However, measurements of NSC using both natural methods and manipulations suffer great uncertainties in testing these two competing hypotheses. First, high carbohydrate

concentrations could be interpreted as a physiological adaptation to the respiration costs during long winters and/or as an adaptation to the high probability of physical damage to tree tissues due to snow accumulation and high winds [22–24]. Second, the experiments with bud treatments or CO_2 manipulations may also induce other changes in tree physiology, such as changes in water relations. For example, water relations [17,25] and nitrogen availability [14,26] change with defoliation. Therefore, a more growth-process-related and less destructive leaf-level indicator is urgently needed.

Stable carbon isotopes ($\delta^{13}C$) and stable oxygen isotopes ($\delta^{18}O$) measured on tree-ring cellulose can provide insights into the changes in photosynthesis, stomatal conductance and transpiration that occur in response to variable growth conditions [27–29]. Stable isotope ratios of carbon, measured as $\delta^{13}C$ values, can be used as an indicator of tree water use response. The photosynthetic carbon isotope discrimination is sensitive to the ratio of CO_2 concentration inside leaves to that outside the leaves (C_i/C_a) [30]. The $\delta^{13}C$ varies as the value of C_i/C_a changes as a function of stomatal conductance (g_s) and photosynthetic activity (A) [30,31]. A combination of tree-ring cellulose $\delta^{13}C$ and $\delta^{18}O$ can be used to tease apart the relative contributions of A and g_s to the $\delta^{13}C$ signal, because the $\delta^{18}O$ signal primarily reflects water fluxes and processes affecting g_s. Therefore, a combination of tree-ring $\delta^{13}C$ and $\delta^{18}O$ along an altitudinal gradient can shed light on tree carbon dynamics and improve our understanding of the physiological mechanisms underlying the treeline formation [32–35].

Here, we present a data set consists of tree-ring width, cellulose $\delta^{13}C$ and $\delta^{18}O$ from Balfour spruce (*Picea likiangensis* var. *rubescens*) and Himalayan fir (*Abies spectabilis*) growing at treeline and lower elevations on the Tibetan Plateau. We combined records of tree-ring $\delta^{13}C$ and $\delta^{18}O$, in order to tease apart photosynthetic activity from leaf–gas exchange of trees at both treelines and low-elevation forests, by applying the theoretical principles of a conceptual dual-isotope model that gives insight into the relationship between stomatal conductance and photosynthetic capacity [36,37]. We intend to test if the treeline trees are carbon source-limited or sink-limited. Specifically, we hypothesize that (i) mean stem radial growth rate at treeline is lower than in low-elevation forests; (ii) rising atmospheric CO_2 concentration would lead to enhanced water use efficiency both at treelines and in low-elevation forests; and (iii) photosynthetic carbon gain is higher at treeline than in low-elevation forests. The interpretation of this data set will provide a novel perspective to test the two competing hypotheses (the source limitation and the sink limitation hypotheses) on treeline formation.

2. Materials and Methods

2.1. Site Conditions and Sampling

The study was conducted in two elevational transects, i.e., the Gubailin transect (GBL, 4450–4530 m) and the Dingjie transect (DJ, 3380–3920 m), situated in the Changdu and Dingjie County, respectively, of the Tibetan Plateau (Figure 1), where the climate is mainly influenced by the Indian Summer Monsoon and Westerlies [38]. Monthly mean temperature ranges from −6 to 10 °C and from −10 to 6 °C, and the total annual precipitation is around 450 mm and 845 mm, with most of it falling in the summer, for the two transects, DJ and GBL, respectively. The climate data are from the CRU TS 4.04 data set (https://catalogue.ceda.ac.uk/uuid/89e1e34ec3554dc98594a5732622bce9, accessed on 10th June 2020).

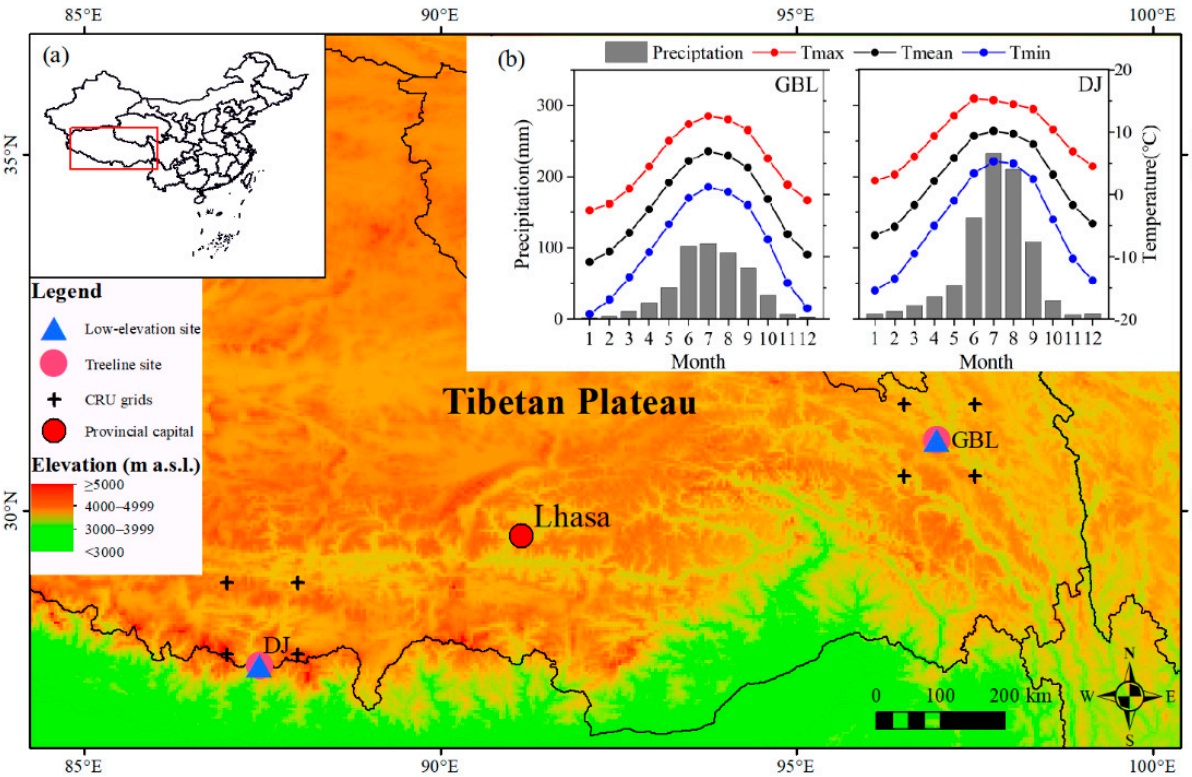

Figure 1. Location map of the two elevational transects on the Tibetan Plateau (**a**), and (**b**) the climate diagrams based on the climate records from the nearest CRU TS 4.04 grids for the period 1955–2014 (https://catalogue.ceda.ac.uk/uuid/89e1e34ec3554dc98594a5732622bce9, accessed on 10th June, 2020). The monthly temperatures include maximum temperature (Tmax), mean temperature (Tmean), minimum temperature (Tmin) and monthly precipitation.

The studied tree species include *Picea likiangensis* var. *rubescens* and *Abies spectabibis*. For the GBL transect, *P. likiangensis* var. *rubescens* forms a pure forest stand in the shady or semi-shady slopes, but in the DJ transect, *A. spectabibis* is the dominant tree species, mixed with other broad-leaf tree species at their lower elevations, and exists as a pure forest at the treeline elevation [39].

Each transect consisted of forest stands of two elevations, i.e., a treeline plot (U) and low-elevation plot (D). Only predominant trees were cored at breast height from a direction parallel to the contour of the slope, one core per tree, using an increment borer with an inner diameter of 5.15 mm. A total of 62 trees were sampled at the GBL transect, including 29 trees from the treeline elevation (GBLU) and 33 from the low-elevation forest (GBLD). At the Dingjie transect, we cored 19 fir trees at the treeline elevation (DJU) and 13 trees from the low-elevation forest (DJD). In total, we sampled 200 tree cores from the alpine treelines and low-elevation forests. These sampling sites were located in remote forests where no evidence of massive human disturbances exists, partly because these forests are under strict protection from logging. There was no clear evidence of fire or other major disturbances.

2.2. Tree-Ring Width Methods

The increment cores were air-dried indoors, mounted on wooden slots, and then polished by progressively finer sandpaper until tree-ring boundaries became clearly visible. With the help of a microscope, tree rings of each sample were cross-dated by comparing the ring patterns among samples. Tree-ring widths were measured by using a LINTAB 6 measuring system with a resolution of 0.001 mm. COFECHA software was used to check visual cross-dating [40]. All the cross-dated ring widths were derived from the ARSTAN software to standardize the ring-width series, using a negative exponential or linear growth curve to eliminate non-climatic signals. The bi-weight robust mean method was used to merge the detrended index series into a standard (STD) chronology for each forest stand.

2.3. Tree-Ring $\delta^{13}C$ and $\delta^{18}O$ Methods

We selected five cores from representative canopy trees at each forest stand that had clear and stiff ring boundaries. Since very thin rings occur for several periods at the treeline sites, the annual rings were pooled from the five samples by combining those from the same year. This pooling method has been proven to be a reliable strategy to extract isotopic signals from tree rings on the southeast Tibetan Plateau [41]. Tree rings with a cambial age of less than 50 years were removed to avoid the effect of juvenile wood on the carbon isotope ratios [42]. To ensure homogeneity and efficiency of α-cellulose extraction, the wood materials were then grounded with a centrifugal mill. We extracted the wood cellulose of annual tree rings following the modified version of the methods [43]. To better homogenize the tree-ring cellulose, we used an ultrasound unit in a hot water bath (JY92-2D, Scientz Industry, Ningbo, China) to disrupt the cellulose [44]. The α-cellulose was then freeze-dried for 72 h using a vacuum freeze dryer (Labconco Corporation, Kansas, MO, USA) before the isotope analysis. The $\delta^{13}C$ values were determined by an element analyzer (Flash EA 1112; Bremen, Germany) coupled with an isotope-ratio mass spectrometer (Delta-plus, Thermo Electron Corporation, Bremen, Germany) at State Key Laboratory of Vegetation and Environmental Change, Institute of Botany Chinese Academy of Sciences. The analytical errors (standard deviations) of the isotope measurements were less than 0.05‰ and 0.3‰ for $\delta^{13}C$ and $\delta^{18}O$, respectively. Calibration was done by measurement of International Atomic Energy Agency (IAEA) USGS-24 (graphite) and by measurement of IAEA-CH_3 (cellulose). All $\delta^{13}C$ and $\delta^{18}O$ values are expressed relative to their respective standard (Vienna Pee Dee Belemnite for carbon isotopes and Vienna Standard Mean Ocean Water for oxygen isotopes).

$$\delta^{13}C = [(R_{sample}/R_{standard}) - 1] \times 1000‰ \quad (1)$$

$R = {}^{13}C/{}^{12}C$; R_{sample} and $R_{standard}$ are the ${}^{13}C/{}^{12}C$ ratios of the samples and the standard, respectively.

To accurately acquire tree ring $\delta^{13}C$, climate change effect, i.e., the increasing trend of atmospheric CO_2 concentration, was removed. We estimated changes in atmospheric CO_2 concentration and ${}^{13}C$ values using ice core's bubble CO_2 concentration, and its $\delta^{13}C$ and monitoring data. The ring carbon isotope fractionation sequence can be calculated through the following equations [30]:

$$\Delta^{13}C = ({}^{13}C_a - {}^{13}C_p)/(1 + {}^{13}C_p/1000) \quad (2)$$

The ${}^{13}C_p$ and ${}^{13}C_a$ in the formula were the ${}^{13}C$ value of $\delta^{13}C$ and CO_2 value of plant photosynthetic products.

$$C_i/C_a = (\Delta^{13}C - a)/(b - a) \quad (3)$$

where a and b represent CO_2 in isotope fractionation during stomatal (4.4‰) carbon isotope fractionation and the RuBP enzyme carboxylation process (27‰). The concentrations of CO_2 in the leaves and CO_2 in the atmosphere were C_i and C_a, respectively. Intrinsic water use efficiency (iWUE) can be estimated using C_i and C_a according to Ehleringer [45]:

$$iWUE = A/g_s = (C_a - C_i)/1.6 \quad (4)$$

where 1.6 is the ratio of diffusivities of water and CO_2 in air.

Given that $\delta^{18}O$ values are a reliable indicator of g_s, the photosynthesis rate could be derived by a transformation of Equation (4):

$$A = iWUE \cdot g_s = iWUE \cdot \delta^{18}O \quad (5)$$

The A is then used to infer the photosynthesis rate for each forest stand compared within each elevational transect.

In this study, the $\delta^{13}C$ series was not detrended because we intended to compare the absolute values among different elevations, rather than infer any trends or correlate with other time series, such as climate variables. However, the significant increase in the atmospheric CO_2 concentrations may affect the comparison of $\delta^{13}C$ and iWUE [33,46]. Therefore, we divided the research period into many slices, with a window-length of approximately 50 years, and then made comparisons over different periods. By doing so, we aimed to see if increased atmospheric CO_2 concentrations have led to different elevational patterns for the compared data. Tree-ring isotopes were measured over the period from 1850 to 2010 for the GBL transect, and from 1900 to 2006 for the DJ transect.

3. Results

3.1. Changes in Tree Growth and Cellulose Stable Isotopes

All chronologies had high SNR (signal-to-noise ratio), SD (standard deviation) and EPS (expressed population signal), indicating that the radial growth of different forest stands was responding to common factors. Moreover, the large percentage of variance explained by the first eigenvectors over the common period indicates that common signals were strong among trees in each forest stand. Additionally, autocorrelations were higher at the treelines than at lower elevations in both transects. Except in DJD, the EPS (expressed population signal) was greater than 0.85 among the studied trees (Table 1).

Table 1. Statistic characteristics of the tree-ring width chronologies. Each of the two transects (GBL and DJ) consisted of forest stands of two elevations, i.e., a treeline plot (U) and low-elevation plot (D).

Statistic Characteristics	GBLU	GBLD	DJU	DJD
Time span	1773–2010	1621–2010	1888–2006	1897–2006
Year since EPS > 0.85	1820–2010	1635–2010	1890–2006	1960–2006
Mean sensitivity	0.105	0.1	0.105	0.1
Standard deviation	0.19	0.173	0.23	0.137
Autocorrelation order 1	0.765	0.761	0.833	0.606
Signal-to-noise ratio *	28.4	33	17.2	10.8
Expressed population signal *	0.94	0.934	0.931	0.72
Variance in first eigenvector (%) *	57	61.1	80.2	41.2
$\delta^{13}C$ and $\delta^{18}O$ time span	1850–2010	1850–2010	1900–2006	1900–2006

* Calculated over the common period 1900–2005.

In general, during the study period, the base area increment (BAI) of the treelines was lower than that at low elevations, but BAI in recent decades was lower in GBLD (Figure 2). Tree-ring $\delta^{13}C$ was higher at low elevations than treelines during the study period (Figure 3). There was no significant difference in $\delta^{18}O$ between treelines and low elevations (Figure 4).

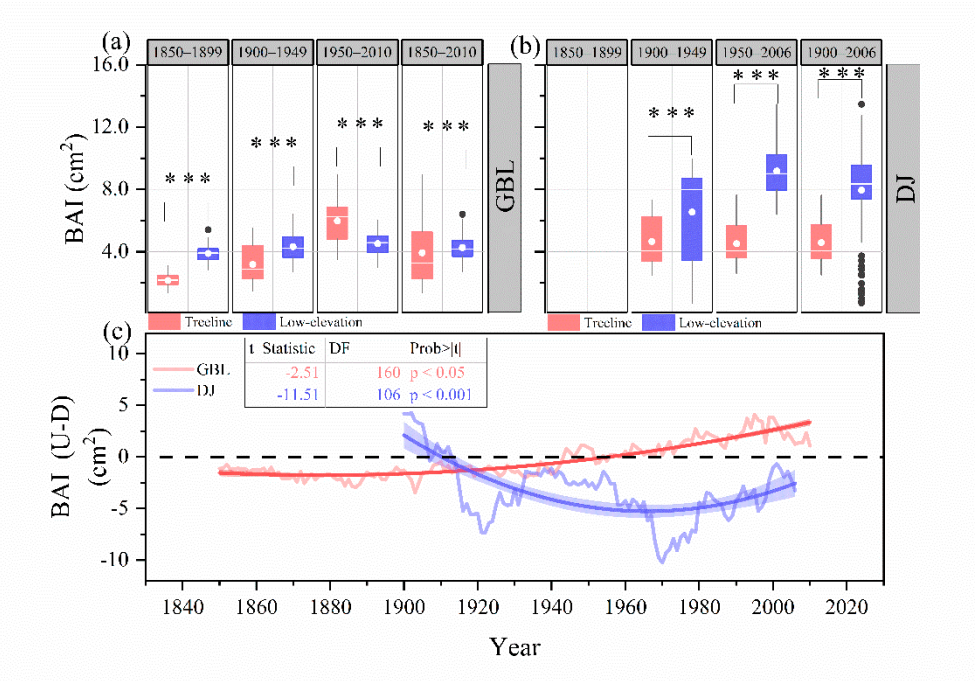

Figure 2. Comparisons of the mean values of tree-ring BAI between the treeline (U) and low-elevation (D) plots for the two elevational transects GBL and DJ over different time periods (**a**,**b**), and (**c**) the difference (U-D) in BAI between treeline and low elevation. The black dots represent outliers as judged by more than 3 standard deviations departed from the mean values. *** denotes significant difference of means between the compared groups at $p < 0.001$ level. The bold lines in (**c**) are regression lines and the shaded area denotes the 95% confidence intervals of the regressions.

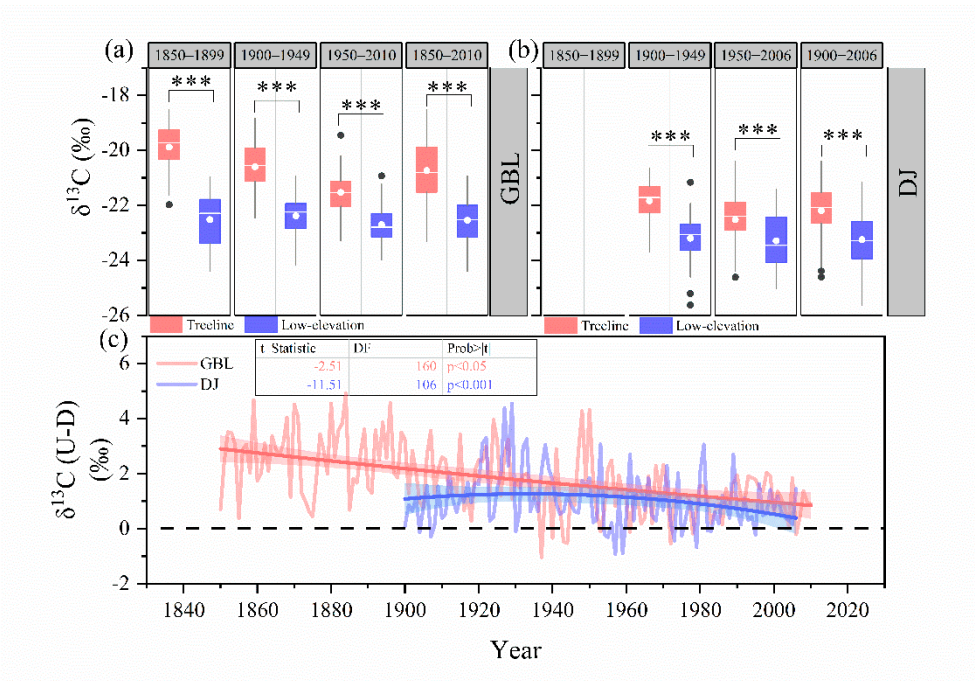

Figure 3. Comparisons of the mean values of tree-ring $\delta^{13}C$ between the treeline (U) and low-elevation (D) plots for the two elevational transects GBL and DJ over different time periods (**a**,**b**), and (**c**) the difference (U-D) in BAI between treeline and low elevation. The black dots represent outliers as judged by more than 3 standard deviations departed from the mean values. *** denotes significant difference of means between the compared groups at $p < 0.001$ level. The bold lines in (**c**) are regression lines and the shaded area denotes the 95% confidence intervals of the regressions.

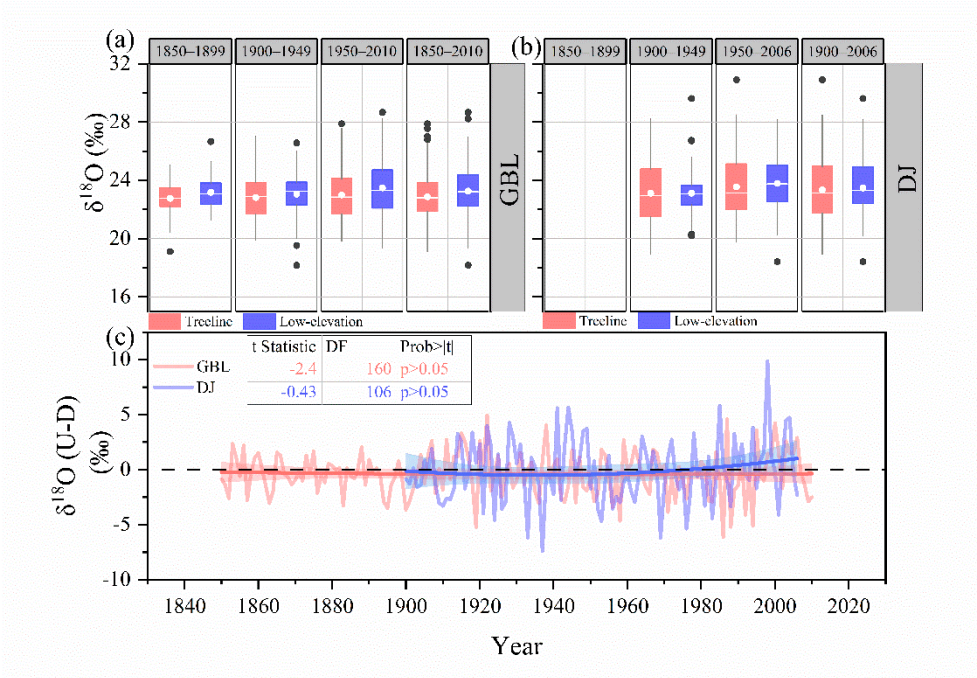

Figure 4. Comparisons of the mean values of tree-ring $\delta^{18}O$ between the treeline (U) and low-elevation (D) plots for the two elevational transects GBL and DJ over different time periods (**a**,**b**), and (**c**) the difference (U-D) in BAI between treeline and low elevation. The black dots represent outliers as judged by more than 3 standard deviations departed from the mean values. The bold lines in (**c**) are regression lines and the shaded area denotes the 95% confidence intervals of the regressions.

3.2. Conceptual Model of $\delta^{13}C$ and $\delta^{18}O$ Relationships

Changes in photosynthetic assimilation rates and/or stomatal conductance in treelines and low-elevation forests were estimated by assessing the shifts in the $\delta^{13}C$–$\delta^{18}O$ space (Figure 5). Comparing the average isotope values of the treelines and low elevations, $\delta^{13}C$ was greater in treelines and low-elevation forests at the GBL and DJ site, while no significant difference was found for $\delta^{18}O$ in treelines and low elevations (Figures 3 and 4). Since $\delta^{18}O$ remained unchanged between the two altitudes, the observed change in $\delta^{13}C$ can only be explained by a higher A, but not by a decrease in g_s (Figure 6), according to the dual-isotope approach of Scheidegger et al. (2000).

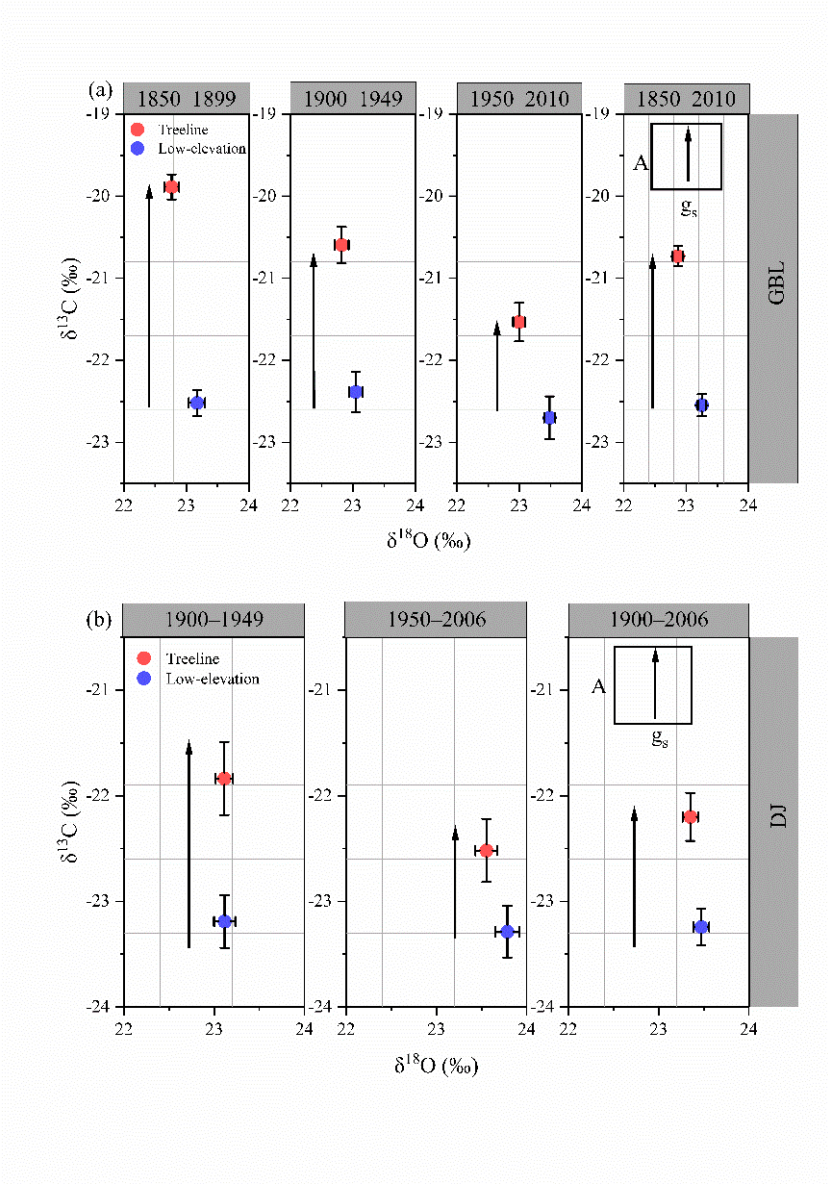

Figure 5. Relationships between $\delta^{13}C$ and $\delta^{18}O$ in treelines vs. low elevations in two species at GBL (**a**) and DJ (**b**) transect. Mean values (symbols) ± 1 SE are shown. Shifts in the isotopic space are represented by arrows. The insets display the relative changes in the corresponding photosynthetic assimilation rate (A) vs. stomatal conductance (g_s) responses, according to the dual-isotope conceptual model. Note that the upward vertical arrows show the increase in the $\delta^{13}C$ from low elevation to treeline over equal or similar $\delta^{18}O$ values, which is a typical scenario of constant stomatal conductance and increasing photosynthesis in the carbon and oxygen double-isotope model [37].

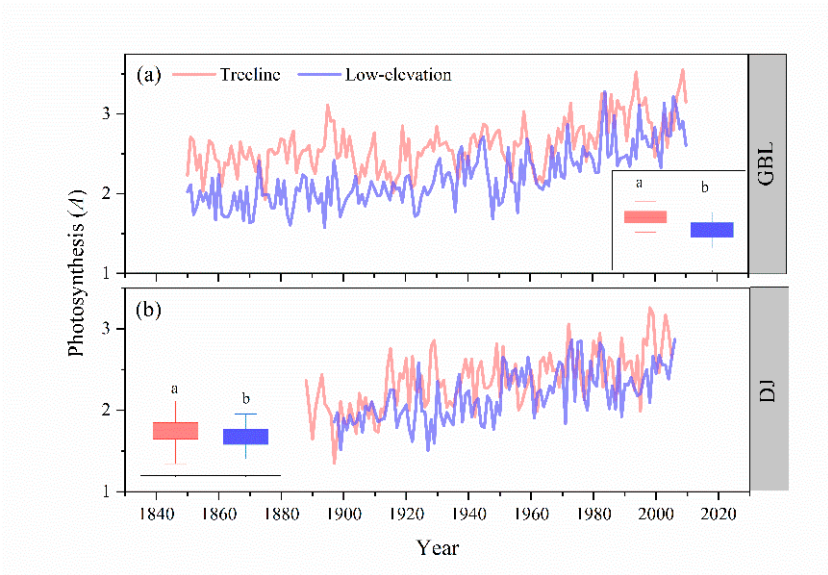

Figure 6. The temporal changes in photosynthesis (A) for each forest stand of the two elevational transects GBL (**a**) and DJ (**b**). The photosynthesis rates are derived from a transformation of Equation (4): $A = iWUE \cdot g_s = iWUE \cdot \delta^{18}O$. Different letters demonstrate significant differences ($p < 0.05$) between treelines and low-elevation forests based on two-tailed two-sample t-tests, assuming equal variance.

4. Discussion

Tree-ring $\delta^{13}C$ is expected to be strongly affected by photosynthetic rates, which are governed both by temperature and by other factors at the upper treeline [35,47,48]. Following the theoretical principles of the dual-isotope model [28], we found that photosynthesis is greater at treeline than at low-elevation forests. The synergistic effect of elevated CO_2 and temperature was reported to stimulate forest productivity in high mountainous forest ecosystems of temperature-limited environments [2,49]. Elevated C_a could improve photosynthesis (A) through the enhanced reaction rate of the RuBisco enzyme [50–52]. Increased A may improve the non-structural carbon (NSC) pool, which could be used for sink activities such as growth [53].

Our results imply that treeline trees are able to acquire photoassimilates so efficiently that growth consumption will not be able to deplete the carbohydrate pool (Figures 2 and 6). Consequently, carbohydrates accumulate in tissues, and trees have more available carbon than sinks are able to consume. Although the carbon status of trees was improved given the increased iWUE and A, such improvement may not translate into tissue growth because such a process was not carbon-limited. Low temperature limits meristematic activity [6]. Therefore, growth ceases at a relatively higher temperature than photosynthesis [7]. It is likely that trees uphold their carbon uptake under warmer conditions because increased CO_2 atmospheric concentrations compensate for reduced stomatal conductance, which occurs more frequently, possibly due to drier conditions [54–58]. Nonetheless, this uptaken carbon may not be translated into enhanced tree growth [34,59,60], but might go to other potential sinks, such as root systems [11,61,62].

The winter respiratory costs in treeline trees usually do not exceed c. 10–15% of the carbon acquired during the growing season [63], and the requirement for carbohydrate storage can be assumed to remain fairly stable in the long term. Cold-adapted tree species reduce stem and shoot growth when the temperature drops below 5–7 °C [64], but their light-saturated photosynthesis still reaches more than 50% of full capacity at such temperatures, and their tissues are fully charged with storage carbohydrates such as starch and soluble sugars [65]. Therefore, when low temperatures constrain tissue production, the rate of photosynthetic assimilate production may exceed demand. An in situ study of *Pinus cembra* at an alpine timberline suggested that total measured carbon loss during

the winter months was small, equaling the photosynthetic production of one to two warm days in spring or summer, when the average air temperature was above 6 °C [63].

Furthermore, we found that tree growth at the two treelines is generally lower than in low-elevation forests, despite the recent increase in growth rate (Figure 2). Rising atmospheric CO_2 concentration stimulates leaf-level photosynthesis, but not growth [34,55,66,67]. Our results show that the increasing CO_2 concentration during the past century did not affect the tree growth. Not only dependent on photosynthesis rate, tree growth can be affected by other factors, such as nutrient availability, which may confound the effects of atmospheric CO_2 enrichment at treelines [68]. Moreover, water is particularly vital for cell elongation [7]. In arid mountains, trees face simultaneously low temperature and drought, strongly restricting their growth [69,70]. A recent study suggests a sink limitation as the main mechanism behind treeline formation in high, arid Himalayas [13].

Overall, our findings suggest a larger photosynthesis rate and smaller growth rate of trees at treelines as compared with low-elevation forests (Figure 6), providing supportive evidence for the growth limitation on treeline formation. Moreover, Tibetan treelines may have great potential to benefit from the ongoing climate warming due to their ability to cope with the co-occurring drought stress through enhanced water use efficiency.

5. Conclusions

This study leveraged tree-ring isotope techniques along two treeline transects on the eastern Tibetan Plateau to provide physiological evidence of the sink limitation on treeline formation. Ring widths are overall narrower at treelines than in low-elevation forests. The cellulose-stable isotopes suggest that higher iWUE was observed at treelines, possibly due to their better ability to cope with warming-related drought stress and rising atmospheric CO_2, as compared with low-elevation forests. Combined with comparable tree-ring $\delta^{18}O$ at treeline and in low-elevation forests, our results further show that photosynthesis is higher at the treeline than at lower elevations, which is supportive evidence for the sink limitation hypothesis on the formation of the upper treeline in the study region. Therefore, we demonstrate that tree-ring isotopes may hold great potential to further elucidate the underlying mechanisms that form the alpine treelines in a new and physiologically meaningful perspective at leaf level.

Author Contributions: X.P. and L.L. conceived the research, X.P. performed the statistical analyses, X.P., L.L. and X.W. wrote the paper. All authors contributed to the interpretation of the results. The authors declare they have no conflicts of interest regarding this article. All authors have read and agreed to the published version of the manuscript.

Funding: This research was funded by the Natural Science Foundation of China (grant number 41771060 and 31870460) and the Open Grant for Key Laboratory of Sustainable Forest Ecosystem Management (Northeast Forestry University), Ministry of Education (grant Number KFJJ2019YB01). The APC was funded by the Institute of Botany, Chinese Academy of Sciences. All authors have read and agreed to the published version of the manuscript.

Institutional Review Board Statement: Not applicable.

Informed Consent Statement: Not applicable.

Data Availability Statement: The data presented in this study are available on request from the corresponding author.

Acknowledgments: We are thankful to Qi-Bin Zhang for the design of the project and supervision of the study. We are grateful to the Tibetan Forestry Bureau for permitting the field sampling.

Conflicts of Interest: The authors declare no conflict of interest.

References

1. Körner, C.; Paulsen, J. A world-wide study of high altitude treeline temperatures. *J. Biogeogr.* **2004**, *31*, 713–732. [CrossRef]
2. Camarero, J.J.; Gazol, A.; Sanchez-Salguero, R.; Fajardo, A.; McIntire, E.J.B.; Gutierrez, E.; Batllori, E.; Boudreau, S.; Carrer, M.; Diez, J.; et al. Global fading of the temperature-growth coupling at alpine and polar treelines. *Glob. Chang. Biol.* **2021**, *27*, 1879–1889. [CrossRef] [PubMed]
3. Lu, X.; Liang, E.; Wang, Y.; Babst, F.; Camarero, J.J. Mountain treelines climb slowly despite rapid climate warming. *Glob. Ecol. Biogeogr.* **2021**, *30*, 305–315. [CrossRef]
4. Susiluoto, S.; Hilasvuori, E.; Berninger, F. Testing the growth limitation hypothesis for subarctic Scots pine. *J. Ecol.* **2010**, *98*, 1186–1195. [CrossRef]
5. Li, M.-H.; Xiao, W.-F.; Wang, S.-G.; Cheng, G.-W.; Cherubini, P.; Cai, X.-H.; Liu, X.-L.; Wang, X.-D.; Zhu, W.-Z. Mobile carbohydrates in Himalayan treeline trees I. Evidence for carbon gain limitation but not for growth limitation. *Tree Physiol.* **2008**, *28*, 1287–1296. [CrossRef]
6. Holtmeier, F.-K.; Broll, G. Treeline Research—From the Roots of the Past to Present Time. A Review. *Forests* **2020**, *11*, 38. [CrossRef]
7. Körner, C. Paradigm shift in plant growth control. *Curr. Opin. Plant Biol.* **2015**, *25*, 107–114. [CrossRef]
8. Hoch, G.; Popp, M.; Körner, C. Altitudinal increase of mobile carbon pools in Pinus cembra suggests sink limitation of growth at the Swiss treeline. *Oikos* **2002**, *98*, 361–374. [CrossRef]
9. Shi, P.; Körner, C.; Hoch, G. End of season carbon supply status of woody species near the treeline in western China. *Basic Appl. Ecol.* **2006**, *7*, 370–377. [CrossRef]
10. Hoch, G.; Körner, C. The carbon charging of pines at the climatic treeline: A global comparison. *Oecologia* **2003**, *135*, 10–21. [CrossRef] [PubMed]
11. Piper, F.I.; Viñegla, B.; Linares, J.C.; Camarero, J.J.; Cavieres, L.A.; Fajardo, A. Mediterranean and temperate treelines are controlled by different environmental drivers. *J. Ecol.* **2016**, *104*, 691–702. [CrossRef]
12. Walker, A.P.; De Kauwe, M.G.; Bastos, A.; Belmecheri, S.; Georgiou, K.; Keeling, R.F.; McMahon, S.M.; Medlyn, B.E.; Moore, D.J.P.; Norby, R.J.; et al. Integrating the evidence for a terrestrial carbon sink caused by increasing atmospheric CO_2. *New Phytol.* **2021**, *229*, 2413–2445. [CrossRef]
13. Dolezal, J.; Kopecky, M.; Dvorsky, M.; Macek, M.; Rehakova, K.; Capkova, K.; Borovec, J.; Schweingruber, F.; Liancourt, P.; Altman, J. Sink limitation of plant growth determines tree line in the arid Himalayas. *Funct. Ecol.* **2019**, *33*, 553–565. [CrossRef]
14. Li, M.-H.; Xiao, W.-F.; Shi, P.; Wang, S.-G.; Zhong, Y.-D.; Liu, X.-L.; Wang, X.-D.; Cai, X.-H.; Shi, Z.-M. Nitrogen and carbon source-sink relationships in trees at the Himalayan treelines compared with lower elevations. *Plant Cell Environ.* **2008**, *31*, 1377–1387. [CrossRef] [PubMed]
15. Honkanen, T.; Haukioja, E.; Suomela, J. Effects of Simulated Defoliation and Debudding on Needle and Shoot Growth in Scots Pine (*Pinus sylvestris*): Implications of Plant Source/Sink Relationships for Plant-Herbivore Studies. *Funct. Ecol.* **1994**, *8*, 631. [CrossRef]
16. Myers, D.A.; Thomas, R.B.; DeLucia, E.H. Photosynthetic Responses of Loblolly Pine (*Pinus Taeda*) Needlesto Experimental Reduction in Sink Demand. *Tree Physiol.* **1999**, *19*, 235–242. [CrossRef] [PubMed]
17. Martínez-Vilalta, J.; Sala, A.; Asensio, D.; Galiano, L.; Hoch, G.; Palacio, S.; Piper, F.I.; Lloret, F. Dynamics of non-structural carbohydrates in terrestrial plants: A global synthesis. *Ecol. Monogr.* **2016**, *86*, 495–516. [CrossRef]
18. Handa, I.T.; Körner, C.; Hättenschwiler, S. Conifer stem growth at the altitudinal treeline in response to four years of CO_2 enrichment. *Glob. Chang. Biol.* **2006**, *12*, 2417–2430. [CrossRef]
19. Guillemot, J.; Martin-StPaul, N.K.; Dufrene, E.; Francois, C.; Soudani, K.; Ourcival, J.-M.; Delpierre, N. The dynamic of the annual carbon allocation to wood in European tree species is consistent with a combined source–sink limitation of growth: Implications for modelling. *Biogeosciences* **2015**, *12*, 2773–2790. [CrossRef]
20. Lyytikäinen-Saarenmaa, P. The responses of scots pine, pinus sylvestris, to natural and artificial defoliation stress. *Ecol. Appl.* **1999**, *9*, 469–474. [CrossRef]
21. Fajardo, A.; Piper, F.I.; Pfund, L.; Körner, C.; Hoch, G. Variation of mobile carbon reserves in trees at the alpine treeline ecotone is under environmental control. *New Phytol.* **2012**, *195*, 794–802. [CrossRef]
22. Tranquillini, W. *Physiological Ecology of the Alpine Treeline*; Springer: Berlin, Germany, 1979.
23. Susiluoto, S.; Perämäki, M.; Nikinmaa, E.; Berninger, F. Effects of sink removal on transpiration at the treeline: Implications for the growth limitation hypothesis. *Environ. Exp. Bot.* **2007**, *60*, 334–339. [CrossRef]
24. Dang, H.S.; Zhang, K.R.; Zhang, Q.F.; Xu, Y.M. Temporal variations of mobile carbohydrates in Abies fargesii at the upper tree limits. *Plant Biol.* **2015**, *17*, 106–113. [CrossRef]
25. Berninger, F.; Sonninen, E.; Aalto, T.; Lloyd, J. Modeling ^{13}C discrimination in tree rings. *Glob. Biogeochem. Cycles* **2000**, *14*, 213–223. [CrossRef]
26. Betson, N.R.; Johannisson, C.; Löfvenius, M.O.; Grip, H.; Granström, A.; Högberg, P. Variation in the δ13C of foliage of Pinus sylvestris L. in relation to climate and additions of nitrogen: Analysis of a 32-year chronology. *Glob. Chang. Biol.* **2007**, *13*, 2317–2328. [CrossRef]
27. McCarroll, D.; Loader, N.J. Stable isotopes in tree rings. *Quat. Sci. Rev.* **2004**, *23*, 771–801. [CrossRef]
28. Sveinbjörnsson, B. North American and European treelines: External factors and internal processes controlling position. *Ambio* **2000**, *29*, 388–395. [CrossRef]

29. Mathias, J.M.; Thomas, R.B. Global tree intrinsic water use efficiency is enhanced by increased atmospheric CO_2 and modulated by climate and plant functional types. *Proc. Natl. Acad. Sci. USA* **2021**, *118*. [CrossRef]
30. Farquhar, G.D.; Ehleringer, J.R.; Hubic, K.T. Carbon isotope discrimination and photosynthesis. *Annu. Rev. Plant Physiol. PlantMol. Biol.* **1989**, *40*, 503–537. [CrossRef]
31. Seibt, U.; Rajabi, A.; Griffiths, H.; Berry, J.A. Carbon isotopes and water use efficiency: Sense and sensitivity. *Oecologia* **2008**, *155*, 441–454. [CrossRef]
32. Guerrieri, R.; Belmecheri, S.; Ollinger, S.V.; Asbjornsen, H.; Jennings, K.A.; Xiao, J.F.; Stocker, B.D.; Martin, M.E.; Hollinger, D.Y.; Brachogarrillo, R.; et al. Disentangling the role of photosynthesis and stomatal conductanceon rising forest water-use efficiency. *Proc. Natl. Acad. Sci. USA* **2019**, *116*, 16909–16914. [CrossRef]
33. Liu, X.; Zhao, L.; Voelker, S.; Xu, G.; Zeng, X.; Zhang, X.; Zhang, L.; Sun, W.; Zhang, Q.; Wu, G.; et al. Warming and CO_2 enrichment modified the ecophysiological responses of Dahurian larch and Mongolia pine during the past century in the permafrost of northeastern China. *Tree Physiol.* **2018**, *39*, 88–103. [CrossRef] [PubMed]
34. Reed, C.C.; Ballantyne, A.P.; Cooper, L.A.; Sala, A. Limited evidence for CO_2-related growth enhancement in northern Rocky Mountain lodgepole pine populations across climate gradients. *Glob. Chang. Biol.* **2018**, *24*, 3922–3937. [CrossRef] [PubMed]
35. Wu, G.; Liu, X.; Chen, T.; Xu, G.; Wang, W.; Zeng, X.; Zhang, X. Elevation-dependent variations of tree growth and intrinsic water-use efficiency in Schrenk spruce (*Picea schrenkiana*) in the western Tianshan Mountains, China. *Front. Plant Sci.* **2015**, *6*, 309. [CrossRef] [PubMed]
36. Barnard, H.R.; Brooks, J.R.; Bond, B.J. Applying the dual-isotope conceptual model to interpret physiological trends under uncontrolled conditions. *Tree Physiol.* **2012**, *32*, 1183–1198. [CrossRef] [PubMed]
37. Scheidegger, Y.; Saurer, M.; Bahn, M.; Siegwolf, R. Linking stable oxygen and carbon isotopes with stomatal conductance andphotosynthetic capacity: A conceptual model. *Oecologia* **2000**, *125*, 350–357. [CrossRef] [PubMed]
38. Yeh, T.C.; Gao, Y.X. *Meteorology of the Qinghai-Xizang (Tibet) Plateau*; Science Press: Beijing, China, 1979. (In Chinese)
39. Xu, L.-X. *Ecology Episode of Xi Zang 50 Year*; National Publishing House: Beijing, China, 2001. (In Chinese)
40. Holmes, R.L. Computer-Assisted Quality Control in Tree-Ring Dating and Measurement. *Tree-Ring Bull.* **1983**, *43*, 51–67.
41. Shi, C.; Masson-Delmotte, V.; Risi, C.; Eglin, T.; Stievenard, M.; Pierre, M.; Wang, X.; Gao, J.; Bréon, F.-M.; Zhang, Q.-B.; et al. Sampling strategy and climatic implications of tree-ring stable isotopes on the southeast Tibetan Plateau. *Earth Planet. Sci. Lett.* **2011**, *301*, 307–316. [CrossRef]
42. Leavitt, S.W. Tree-ring C–H–O isotope variability and sampling. *Sci. Total Environ.* **2010**, *408*, 5244–5253. [CrossRef]
43. Loader, N.J.; Robertson, I.; Barker, A.C.; Switsur, V.R.; Waterhouse, J.S. An improved technique for the batch pro-cessing of small wholewood samples to α-cellulose. *Chem. Geol.* **1997**, *136*, 313–317. [CrossRef]
44. Laumer, W.; Andreu, L.; Helle, G.; Schleser, G.H.; Wieloch, T.; Wissel, H. A novel approach for the homogenization of cellulose to use micro-amounts for stable isotope analyses. *Rapid Commun. Mass Spectrom.* **2009**, *23*, 1934–1940. [CrossRef] [PubMed]
45. Ehleringer, J.R. Carbon and Water Relations in Desert Plants: An Isotopic Perspective. In *Stable Isotopes and Plant Carbon-Water Relations*; Ehleringer, J.R., Hall, A.E., Farquhar, G.D., Eds.; Academic Press: London, UK, 1993; pp. 155–172.
46. Wu, G.; Liu, X.; Chen, T.; Xu, G.; Wang, W.; Zeng, X.; Wang, B.; Zhang, X. Long-term variation of tree growth and intrinsic water-use efficiency in Schrenk spruce with increasing CO_2 concentration and climate warming in the western Tianshan Mountains, China. *Acta Physiol. Plant.* **2015**, *37*, 150. [CrossRef]
47. Panthi, S.; Fan, Z.; Van Der Sleen, P.; Zuidema, P.A. Long-term physiological and growth responses of Himalayan fir to environmental change are mediated by mean climate. *Glob. Chang. Biol.* **2019**, *26*, 1778–1794. [CrossRef] [PubMed]
48. Sigdel, S.R.; Wang, Y.; Camarero, J.J.; Zhu, H.; Liang, E.; Peñuelas, J. Moisture-mediated responsiveness of treeline shifts to global warming in the Himalayas. *Glob. Chang. Biol.* **2018**, *24*, 5549–5559. [CrossRef] [PubMed]
49. Salzer, M.W.; Hughes, M.K.; Bunn, A.G.; Kipfmueller, K.F. Recent unprecedented tree-ring growth inbristlecone pine at the highest elevations and possible causes. *Proc. Nat. Acad. Sci. USA* **2009**, *106*, 20348–20353. [CrossRef]
50. Ainsworth, E.A.; Rogers, A. The response of photosynthesis and stomatal conductance to rising [CO_2]: Mechanisms and environmental interactions. *Plant Cell Environ.* **2007**, *30*, 258–270. [CrossRef] [PubMed]
51. Haverd, V.; Smith, B.; Canadell, J.G.; Cuntz, M.; Mikaloff-Fletcher, S.; Farquhar, G.; Woodgate, W.; Briggs, P.R.; Trudinger, C.M. Higher than expected CO_2 fertilization inferred from leaf to global observations. *Glob. Chang. Biol.* **2020**, *26*, 2390–2402. [CrossRef]
52. Huang, J.-G.; Bergeron, Y.; Denneler, B.; Berninger, F.; Tardif, J. Response of Forest Trees to Increased Atmospheric CO_2. *Crit. Rev. Plant Sci.* **2007**, *26*, 265–283. [CrossRef]
53. Streit, K.; Siegwolf, R.T.W.; Hagedorn, F.; Schaub, M.; Buchmann, N. Lack of photosynthetic or stomatal regulation after 9 years of elevated [CO_2] and 4 years of soil warming in two conifer species at the alpine treeline. *Plant Cell Environ.* **2013**, *37*, 315–326. [CrossRef]
54. Silva, L.C.R.; Horwath, W.R. Explaining Global Increases in Water Use Efficiency: Why Have We Overestimated Responses to Rising Atmospheric CO_2 in Natural Forest Ecosystems? *PLoS ONE* **2013**, *8*, e53089. [CrossRef]
55. Martínez-Sancho, E.; Dorado-Liñán, I.; Merino, E.G.; Matiu, M.; Helle, G.; Heinrich, I.; Menzel, A. Increased water-use efficiency translates into contrasting growth patterns of Scots pine and sessile oak at their southern distribution limits. *Glob. Chang. Biol.* **2017**, *24*, 1012–1028. [CrossRef]
56. Lévesque, M.; Siegwolf, R.; Saurer, M.; Eilmann, B.; Rigling, A. Increased water-use efficiency does not lead to en-hanced tree growth under xeric and mesic conditions. *New Phytol.* **2014**, *203*, 94–109. [CrossRef] [PubMed]

57. Gómez-Guerrero, A.; Silva, L.C.R.; Barrera-Reyes, M.; Kishchuk, B.; Velázquez-Martínez, A.; Martínez-Trinidad, T.; Plascencia-Escalante, F.O.; Horwath, W.R. Growth decline and divergent tree ring isotopic composition (δ13C and δ18O) contradict predictions of CO_2 stimulation in high altitudinal forests. *Glob. Chang. Biol.* **2013**, *19*, 1748–1758. [CrossRef] [PubMed]
58. Fajardo, A.; Gazol, A.; Mayr, C.; Camarero, J.J. Recent decadal drought reverts warming-triggered growth en-hancement in contrasting climates in the southern Andes tree line. *J. Biogeogr.* **2019**, *46*, 1367–1379.
59. Peñuelas, J.; Canadell, J.G.; Ogaya, R. Increased water-use efficiency during the 20th century did not translate into enhanced tree growth. *Glob. Ecol. Biogeogr.* **2010**, *20*, 597–608. [CrossRef]
60. Peters, W.; Van Der Velde, I.R.; Van Schaik, E.; Miller, J.B.; Ciais, P.; Duarte, H.F.; Van Der Laan-Luijkx, I.T.; Van Der Molen, M.K.; Scholze, M.; Schaefer, K.; et al. Increased water-use efficiency and reduced CO_2 uptake by plants during droughts at a continental scale. *Nat. Geosci.* **2018**, *11*, 744–748. [CrossRef] [PubMed]
61. Piper, F.I.; Fajardo, A.; Hoch, G. Single-provenance mature conifers show higher non-structural carbohydrate storage and reduced growth in a drier location. *Tree Physiol.* **2017**, *37*, 1001–1010. [CrossRef]
62. Muller, B.; Pantin, F.; Génard, M.; Turc, O.; Freixes, S.; Piques, M.; Gibon, Y. Water deficits uncouple growth from photosynthesis, increase C content, and modify the relationships between C and growth in sink organs. *J. Exp. Bot.* **2011**, *62*, 1715–1729. [CrossRef]
63. Wieser, G. Carbon dioxide gas exchange of cembran pine (*Pinus cembra*) at the alpine timberline during winter. *Tree Physiol.* **1997**, *17*, 473–477. [CrossRef]
64. Rossi, S.; DesLauriers, A.; Griçar, J.; Seo, J.-W.; Rathgeber, C.B.; Anfodillo, T.; Morin, H.; Levanic, T.; Oven, P.; Jalkanen, R. Critical temperatures for xylogenesis in conifers of cold climates. *Glob. Ecol. Biogeogr.* **2008**, *17*, 696–707. [CrossRef]
65. Körner, C.; Riedl, S. *Alpine Treelines: Functional Ecology of the Global High Elevation Tree Limits*; Springer: Basel, Switzerland, 2012; p. 357.
66. Girardin, M.P.; Bouriaud, O.; Hogg, E.H.; Kurz, W.; Zimmermann, N.E.; Metsaranta, J.M.; Jong, R.; Frank, D.C.; Esper, J.; Buntgen, U.; et al. No growth stimulation of Canada's boreal forets under half-century of combined warming and CO_2 fertilization. *Proc. Natl. Acad. Sci. USA* **2016**, *113*, E8406–E8414. [CrossRef]
67. Giguère-Croteau, C.; Boucher, É.; Bergeron, Y.; Girardin, M.P.; Drobyshev, I.; Silva, L.C.R.; Hélie, J.-F.; Garneau, M. North America's oldest boreal trees are more efficient water users due to increased [CO_2], but do not grow faster. *Proc. Natl. Acad. Sci. USA* **2019**, *116*, 2749–2754. [CrossRef] [PubMed]
68. Silva, L.C.R.; Anand, M. Probing for the influence of atmospheric CO_2 and climate change on forest ecosystems across biomes. *Glob. Ecol. Biogeogr.* **2012**, *22*, 83–92. [CrossRef]
69. Lyu, L.; Zhang, Q.-B.; Pellatt, M.G.; Büntgen, U.; Li, M.-H.; Cherubini, P. Drought limitation on tree growth at the Northern Hemisphere's highest tree line. *Dendrochronologia* **2019**, *53*, 40–47. [CrossRef]
70. Liang, E.; Dawadi, B.; Pederson, N.; Eckstein, D. Is the growth of birch at the upper timberline in the Himalayas limited by moisture or by temperature? *Ecology* **2014**, *95*, 2453–2465. [CrossRef]